Atmos. Chem. Phys. Discuss., 4, 1887–1909, 2004
www.atmos-chem-phys.org/acpd/4/1887/
SRef-ID: 1680-7375/acpd/2004-4-1887


Atmospheric Chemistry and Physics Discussions

# Heterogeneous freezing of single sulphuric acid solution droplets: laboratory experiments utilising an acoustic levitator

**M. Ettner**[1], **S. K. Mitra**[1], **and S. Borrmann**[1,2]

[1]Institute for Atmospheric Physics, Johannes Gutenberg-University, Mainz, Germany
[2]Max Planck Institute for Chemistry, Mainz, Germany

Received: 23 January 2004 – Accepted: 14 February 2004 – Published: 25 March 2004

Correspondence to: M. Ettner (ettner@mpch-mainz.mpg.de)

## Abstract

The heterogeneous freezing temperatures of single binary sulphuric acid solution droplets were measured in dependency of acid concentration down to temperatures as low as −70°C. In order to avoid influence of supporting substrates on the freezing characteristics, the droplets were suspended by means of an acoustic levitator. The droplets contained immersed particles of graphite, kaolin or montmorillonite in order to study the influence of the presence of such contamination on the freezing temperature. The radii of the suspended droplets spanned the range between 0,4 and 1,1 mm and the concentration of the sulphuric acid solution varied between 5 and 25 weight percent. The presence of the particles in the solution raises the freezing temperature with respect to homogeneous freezing of these solution droplets. The pure solution droplets can be supercooled up to 40° below the ice-acid solution thermodynamic equilibrium curve. Depending on the concentration of sulphuric acid and the nature of the impurity the polluted droplets froze between −11°C and −35°C. The experimental set-up, combining a deep freezer with a movable ultrasonic levitator and suitable optics, proved to be a useful approach for such investigations on individual droplets.

## 1. Introduction

Sulphuric acid is one of the major components of existing particles in the upper troposphere (UT) and lower stratosphere (LS) (Sheridan et al., 1994; Murphy et al., 1998). The emission of sulphur containing gases and their subsequent oxidation produces $H_2SO_4$ in the atmosphere. Droplets, consisting of sulphuric acid/water solution, are often found in a supercooled metastable state.

The atmosphere contains aerosol particles, which could contaminate the aqueous droplets and therefore cause heterogeneous contact or immersion freezing. Clay minerals and carbonaceous particles were often found in the upper troposphere and lower stratosphere (Mason, 1960; Hoffer, 1961; Pueschel et al., 1992). Ice nucleation of wa-



ACPD

4, 1887–1909, 2004

ter in the immersion and contact mode caused by these particles, has been studied by Mason (1960), Hoffer (1961), Pitter and Pruppacher (1973), and Diehl et al. (1998). Also the influence of biogenic materials as pollen and bacteria on the freezing behaviour of solution droplets was measured by (Diehl et al., 2002; von Blohn, 2003).

Emissions of soot particles and sulphate aerosol in the upper troposphere/lower stratosphere by aircraft engines cause the formation of contrails. Such contrails influence the radiative forcing of the atmosphere by reducing the solar radiation and trapping parts of the longwave radiation from earth's surface (Penner et al., 1999). They also have an effect on cirrus cloud formation because gas phase and particulate emissions as well as long-lived contrails sometimes contribute to the formation or persistence of cirrus clouds.

Binary heterogeneous nucleation and condensation produces a coating of liquid $H_2SO_4/H_2O$ on soot particles emitted by aircraft engines. These particles grow by condensation of gaseous $H_2O$ and $H_2SO_4$ and also by coagulation with volatile $H_2SO_4/H_2O$ particles forming a mixed $H_2SO_4/H_2O$-soot aerosol (Penner et al., 1999). Freezing of those particles creates ice particles which form the visible part of the contrails.

The transition from the liquid into the ice phase takes place either through heterogeneous ice nucleation at the interface of the nucleus and the liquid, or by homogeneous nucleation occuring in the interior of the liquid. Here it needs to mentioned, that some recent theoretical studies indicate that the surface of the liquid is a possible site for the initiation of homogeneous nucleation (Tabazadeh et al., 2002).

In the past, numerous studies have been carried out to investigate the homogeneous nucleation of sulphuric acid/water solutions (Bertram et al., 1996; Carleton et al., 1997; Koop et al., 1997, 1998; Krämer, 1998; Prenni et al., 1999; Vortisch et al., 2000). According to these, homogeneous ice nucleation occurs at temperatures significantly below the equilibrium temperature where ice and sulphuric acid solution co-exist.

The efficiency of soot (DeMott et al., 1990, 1999), solid $(NH_4)_2SO_4$, solid $NH_4HSO_4$ (Zuberi et al., 2001), kaolinite and montmorillonite (Zuberi et al., 2002) for causing

heterogeneous ice nucleation in comparison to the homogeneous process has been demonstrated recently.

In this paper, we present laboratory measurements of the freezing behaviour of single, large sulphuric acid/water droplets obtained by using an acoustic levitator in connection with a deep freezer. This technology is briefly described and measured results are presented for homogeneous and heterogeneous freezing temperatures in the immersion mode. Here the freezing was triggered by insoluble particles consisting of kaolin, montmorillionite and graphite (as proxy for soot) added to the droplets. Having size diameters between 400 $\mu$m and 1.1 mm the droplets used in this study are orders of magnitudes larger than the sub-micron to micron sized droplets typically present in the UT/LS. This size range was chosen for the experiments, because higher nucleation rates result. The "volume advantage" is then expected to reduce observation time until a freezing event occurs. Furthermore within this size range evaporation losses of the solution droplet during the observation period are minimised.

## 2. Experimental methodology

The experimental set-up is shown in Fig. 1. A large chest freezer, which can be cooled down to −85°C, houses the closed chamber with the acoustic levitator. Using an elevator mechanism, the levitator unit can be moved from outside of the freezer to its bottom, where the lowest temperatures are encountered. Two CCD-cameras record images of the droplet onto a video tape. One camera is positioned on the top of the freezer, where it records the injection of the droplet into its floating position at an acoustic node. The other CCD-camera is located inside the chest freezer and is protected by a thermally isolated and heated box to ensure its operation at these temperature extremes. The oscillatory motion in the standing sound wave field and the evaporation of the droplet during its cooling down to the freezing point can be visually observed on a monitor and later analysed.

As long as the levitator is moving down to the bottom of the freezer, no images of



ACPD
4, 1887–1909, 2004

the sample can be taken and for this time period of about 2–3 min, the droplet can not be observed. During this period the droplet position can not be externally controlled, which leads to frequent losses of droplets.

The acoustic levitator device used to freely suspend the droplets is shown in Fig. 2.

Inside the acoustic levitator a piezoelectric oscillator (radiator) generates a sound wave at 58 kHz, which is reflected by a concave Teflon reflector. With proper positioning of the reflector, standing waves are produced in the space between the radiator and the reflector. A droplet with a diameter up to 3 mm or as small as 100 $\mu$m can be levitated in a vertical position slightly below the third of the five existing nodes. As the acoustic field strength required to suspend the droplets increases quadratically with its weight, very large droplets can not be levitated. Smaller droplets will evaporate rapidly and cannot be seen clearly with the current magnification of the cameras.

The experimental characteristics are summarised in Table 1. The gravitation force $F_{Grav}$ (in N) is in balance with the axial levitation force $F_{Lev}$ (in N) and the droplet is kept afloat there in a stable position. If the droplet moves horizontally, the gas flow on the side of the droplet towards the levitation axis is higher then on its other side. The resulting underpressure forces the droplet back into its original, stable position. The balance of forces is described by the following equation:

$$F_{Lev} = \frac{5}{6} k\pi \frac{p^2}{\rho_0 c_0^2} r_d^3 \sin(2k\Delta z) = \frac{4}{3}\pi r_d^3 \rho_d g = F_{Grav} \quad (1)$$

The wave number of the sound wave is denoted by k in 1/m, p is the amplitude of sound pressure in N/m$^2$, $r_d$ the radius of the drop in m, $c_0$ the speed of sound in m/s, $\rho_0$ and $\rho_d$ the density of air (0) and the density of the droplet (d) in kg/m$^3$. $\Delta z$ is the vertical displacement from the exact nodal position, and g is the gravitational acceleration in m/s$^2$. The operator controls a micrometer screw by means of a stepper motor, which is used to move the reflector in order to change the distance between the oscillator-radiator and the reflector. This is necessary, because with decreasing temperature the speed of sound and with it the wavelength and thus the separation



ACPD
4, 1887–1909, 2004

between the nodes change. This variation can be compensated with an appropriate reduction of the distance between the radiator and the reflector. For this reason the operator has to observe the experiment using the video images and adjust the sound-field. The micrometer screw has to be heated, because otherwise the lubricating oil will freeze blocking any adjustments. In order to avoid fast temperature changes, the trap is surrounded by a Plexiglass hood. Fluctuating temperatures will otherwise lead to an irreversible deviation of the droplet from its equilibrium position because of the inherent slow operator response time for readjusting the nodal positions resulting a loss of the droplets. A Pt-100 sensor next to the floating droplet allows one to measure a proxy for the droplet temperature. The ultrasonic fields heat the droplet by approximately 2°C. A second temperature sensor is positioned very close to the wall of the Plexiglass hood. The presence of the Plexiglass hood allows the temperature of the drop to decrease at a controlled rate thus enabling the droplet's continuous levitation. A typical temperature record from an experiment is shown in Fig. 3.

Both temperatures decrease, when the acoustic levitator is moved into the freezer. They approach the temperature of the freezer in a certain time, depending on the pre-set freezer temperature. The "droplet temperature" measured with sensor 1, which is illustrated with the red line in Fig. 3, is corrected by 2°C, considering the warming caused by the ultrasonic field. The temperature recorded by sensor 1 in the moment when freezing occurs is regarded as the freezing temperature of the droplet.

At the beginning of the experiment a syringe with a special needle is used to place the solution droplet at the ultrasonic standing wave node, where it is levitated. The needle is teflon-coated to ensure easy detachment of the drop from its tip.

By means of this levitation-technique, we were able to experiment with droplets in the mm size range. Although this relatively large size reduces the effect of evaporation loss, the volume decrease is not negligible. Especially in the beginning of the experiment, the solution is exposed to warmer ambient temperatures, which cause faster evaporation.

To monitor the changing droplet volume continuously during an experiment, the video

images were digitised. In post-processing of each freezing experiment the height and the width of the droplets were determined using the digital images while assuming the droplets to have the shape of rotationally symmetric ellipsoids. Taking this into account the droplet volumes could be obtained from the digitised video images. The assumption of the rotationally symmetric shape of a levitated droplet can be confirmed visually.

Examples for typical droplet images are given in Fig. 4. The left picture shows an unfrozen, liquid sulphuric acid solution droplet containing black graphite particles. The particles inside the liquid rotate due to internal circulation of the droplet induced by the sound waves. The large dark and the white areas result from reflections and refractions from parts of the experimental apparatus. The image to the right shows a frozen droplet with graphite particles on its surface. The transition from the liquid to the solid phase is easily detected from the rapid change of the drop image from transparent to opaque.

Sulphuric acid solutions with initial concentrations of 5, 9 and 11 wt % were investigated. Water from the solution droplets evaporates during each experiment. With the assumption that no $H_2SO_4$evaporates, the concentration of sulphuric acid in the solution increases during the experiment. The actual concentration in the droplet can be calculated with the known decrease of the volume and the density of the solution at the particular temperature (Luo et al., 1996).

To obtain the concentration at the moment of freezing, the volume right before the phase transition is obtained. From the 25 frame-per-second video, the drop volumes were obtained which together with the knowledge of the density of the solutions lead to the determination of the sulphuric acid concentration in the drop.

To investigate heterogeneous ice nucleation, various commercially available materials were added to the solution droplets. The investigated materials, namely graphite, kaolin, montmorillonite KSF and montmorillonite K10, were all obtained in very fine powdered form. The particles were introduced into the droplet simply by dipping the needle tip into the respective substance and then squeezing a volume of the liquid into the acoustic node. The disadvantage of this technique is, that we were not able to determine the number of particles present in the droplet.



ACPD
4, 1887–1909, 2004

## 3. Sources of errors

The homogeneous freezing temperature of a liquid depends on the purity of the solution. In order to obtain homogeneous ice nucleation it is of great importance to ensure a high purity of the solution. Because the suspended droplet is more or less exposed to the ambient atmosphere, particles and gases are able to contaminate the solution.

The same precautions are also required for experiments on heterogeneous nucleation. Furthermore, the indefinable number of particles which are brought into the droplet, may influence the freezing behaviour of the droplets. Further technical refinements are currently implemented in order to reduce these effects.

The accuracy of the temperature measurement is 1°C. The error in size determination of the droplet leads to an uncertainty of the volume, which is lower than 5%. The volume error leads to an uncertainty in the calculation of the sulphuric acid concentration.

## 4. Results

Figure 5a shows a typical volume decrease of 2 droplets during exposure inside the trap where the droplet size decreases with time due to evaporation loss of water. This evaporation loss slows down as the temperature of the drop falls with time. At the moment of freezing, the volume of the droplets shows a small jump, which is caused by the transition from the liquid phase to the ice phase. Figure 5b on the right shows a typical increase of the calculated sulphuric acid concentration in the solution droplet with time, caused by the evaporation of water. The error bars result from the uncertainties in the volume measurements. The heterogeneous freezing temperatures in the immersion mode, measured with the ultrasonic levitator device, were higher compared to the homogeneous freezing temperatures of the pure liquid.

Figures 6 and 7 show the freezing temperatures of the single sulphuric acid solution droplets in relation to their concentration. The red circles in Fig. 6 represent the



ACPD

4, 1887–1909, 2004

homogeneous freezing of the pure solution. The green triangles show the solution polluted with graphite particles, whereas the blue triangles presents the solution polluted with montmorillonite KSF. The solid line indicate the phase transition equilibrium between ice and sulphuric acid/water solution (Gable et al., 1950). In the concentration range between 6–8 wt %, the pure solution can be supercooled down to −33°C. With the presence of graphite the freezing temperature increases by 5–6°C. Montmorillonite KSF-particles in the droplet lead to freezing temperatures 20°C higher than that of the pure solution. The two measurements with the lowest freezing temperatures containing graphite are probably frozen homogeneously, because only few particles in the droplets were observed. This indicates the need for further experiments for which droplets with known numbers of contaminating particles are prepared. Figure 7 shows a diagram similar to that in Fig. 6, where the green squares represent the droplets containing kaolin and the blue squares those containing montmorillonite K-10. The detailed data showing freezing temperatures as a function of the sulphuric acid content and the droplet volumes are listed in Table 2 together with estimation of the experimental errors.

## 5. Conclusions

We presented in this paper a contact-less technique to investigate ice nucleation of supercooled droplets. The freezing experiments with sulphuric acid have shown that the pure solution droplets freeze at lower temperatures compared to the heterogeneous freezing temperatures of the polluted droplets. Mineral particles, which are produced in the large desert areas and are transported in the upper troposphere, are able to influence the freezing behaviour of cloud droplets. Soot particles that are directly emitted from aircraft engines into the UT/LS, can also influence the freezing of cloud droplets. This could be of importance for the microphysics of UT/LS-clouds containing supercooled droplets or mixed phase clouds.

By means of this levitation technique we are able to simulate the freezing processes



ACPD
4, 1887–1909, 2004

which are responsible for contrail development (Penner et al., 1999). We are able to investigate the influence of different kinds of aerosols to the immersion freezing of droplets. Furthermore, organic substances can be added to the droplets, which change their surface tension and because of that (might) have influence on their freezing characteristics. Another application of the levitator is the investigation of ice nucleation in the contact mode. The aerosol particles can be brought in the surrounding of the droplet and induce contact freezing, when the particle hit the droplets surface. The visualisation of the freezing process itself will be possible after some optical rearrangements. This will contribute to recently raised issues in the literature concerning the initiation of the freezing process from the interior or the surface of the droplet. Also the studies on the influence of organic surfactants on the freezing can be performed. Thus this small device represents a technique of considerable potential for single droplet experiments.

*Acknowledgements.* This work in part was financially supported by the BMBF (01LO9523/6). We thank B. Luo for his code to determine the density for the sulphuric acid solution.

Edited by: S. T. Martin

## References

Bertram, A. K., Patterson, D. D., and Sloan, J. J.: Mechanisms and temperatures of the freezing of sulphuric acid and aerosols measured by FTTR extinction spectroscopy, J. Phys. Chem., 103, 2376–2383, 1996.

Carleton, K., Sonnenfroh, D., Rawlins, W., Wyslouzil, B., and Arnold, S.: Freezing behaviour of single sulphuric acid aerosols suspended in a quadrupole trap, J. Geophys. Res., 102, 6025, 1997.

DeMott, P. J.: An exploratory-study of ice nucleation by soot aerosols, J. Appl. Meteor., 29, 1072–1079, 1990.

DeMott, P. J., Chen, Y., Kreidenweis, S. M., Rogers, D. C., and Sherman, D. E.: Ice formaton by black carbon particles, Geophys. Res. Lett., 26, 2429–2432, 1999.

Diehl, K. and Mitra, S. K.: A laboratory study of the effects of a kerosene burner exhaust on ice nucleation and evaporation of ice crystals, Atmos. Environ., 32, 3145–3151, 1998.
Diehl, K., Matthias-Maser, S., Mitra, S. K., and Jaenicke, R.: The ice nucleating ability of pollen, Part II: Laboratory studies in immersion and contact freezing modes, Atmos. Res., 61, 125–133, 2002.
Gable, C. M., Betz, H. F., and Maron, S. H.: Phase equilibria of the system sulphuric trioxide-water, J. Amer. Chem. Soc., 72, 1445–1448, 1950.
Hoffer, T.: A laboratory investigation of droplet freezing, J. Met. , 18, 766–778, 1961.
Koop, T., Huey, P. Ng., Molina, L. T., and Molina, M. J.: A new technique to study aerosol phase transitions: the nucleation of ice from $H_2SO_4$ aerosols, J. Phys. Chem. A, 102, 8924–8931, 1998.
Koop, T., Luo, B., Biermann, U., Crutzen, P, and Peter, T.: Freezing of $HNO_3/H_2SO_4/H_2O$ solutions at stratospheric temperatures: nucleation statistics and experiments, J. Phys. Chem., 101, 1117–1133, 1997.
Krämer, B.: Laboruntersuchungen zum Gefrierprozess in polaren Stratosphären-wolken, Dissertation, FU Berlin, 1998.
Luo, B. P., Krieger, U. K., and Peter, T.: Densities and refractive indices of $H_2SO_4/HNO_3/H_2O$ solutions to stratospheric temperatures, Geophys. Res. Lett., 23, 25, 3707–3710, 1996.
Mason, B.: Ice-nucleating properties of clay minerals and stony meteorites, Quart. J. Roy. Meteor. Soc., 86, 552–556, 1960.
Murphy, D. M., Thomson, D. S., and Mahoney, M. J.: In-situ measurements of organics, meteoritic material, mercury, and other elements in aerosols at 5 to 19 kilometers, Science, 282, 1664–1669, 1998.
Penner, J. E., Lister, D. H., Griggs, D. J., Dokken, D. J., and McFarland, M.: Aviation and the global atmosphere, Intergovernmental Panel on Climate Changes, Cambridge University Press, 1999.
Pitter, R. and Pruppacher, H. R.: A wind tunnel investigation of freezing of small water drops falling at terminal velocity in air, Quart. J. Roy. Meteor. Soc., 99, 540–550, 1973.
Prenni, A. J., Wise, M. E., Brooks, S. D., and Tolbert, M. A.: Ice nucleation in sulphuric acid and ammonium sulfate particles, J. Geophys. Res., 106, 3037–3044, 2001.
Pueschel, R. F., Blake, D., Snetsinger, K., Hansen, A. D. A., Verma, S., and Kato, K.: Black carbon (soot) aerosol in the lower stratosphere and upper troposphere, Geophys. Res. Lett., 19, 1659–1662, 1992.



ACPD
4, 1887–1909, 2004

Sheridan, P., Brock, L., and Wilson, J.: Aerosol particles in the upper troposphere and lower stratosphere: Elemental composition and morphology of individual particles in northern latitudes, Geophys. Res. Lett., 21, 2587–2590, 1994.

Tabazadeh, A., Djikaev, Y. S., and Reiss, H.: Surface crystallization of supercooled water in clouds, Proc. Natl. Acad. Sci., 99, 25, 15 873–15 878, 2002.

Von Blohn, N.: Experimentelle Untersuchungen der Eiskeimfähigkeit verschiedener Pollenarten im Immersions- und Kontaktgefrierprozeß, Diploma Thesis, Institut für Physik der Atmosphäre, Mainz, 60–68, 2003.

Vortisch, H., Krämer, B., Weidinger, I., Wöste, L., Leisner, T., Schwell, M., Baumgärtel, H., and Rühl, E.: Homogeneous freezing nucleation rates and crystallization dynamics of single levitated sulphuric acid solution droplets, Phys. Chem. Chem. Phys., 2, 1407–1413, 2000.

Zuberi, B., Bertram, A. K., Koop, T., Molina, L. T, and Molina, M.: Heterogeneous freezing of aqueous particles induced by crystallized $(NH_4)_2SO_4$, ice and letovicite, J. Phys. Chem., 105, 6458–6464, 2001.

Zuberi, B., Bertram, A. K., Cassa, C. A., T., Molina, L. T, and Molina, M.: Heterogeneous nucleation of ice in $(NH_4)_2SO_4$-$H_2O$ particles with mineral dust immersions, Geophys. Res. Lett., 29, doi:10.1029/2001GL014289, 2002.

**Table 1.** Characteristics of the instrumental setup.

| | Applied for this study | Experimentally possible |
|---|---|---|
| Droplet size (mm) | 0.8–2.2 | 0.1–3 |
| Concentration range (wt %) | 5–25 | 0–100 |
| Measurement time (h) | 0.5–4 | 0–unlimited |



ACPD

4, 1887–1909, 2004

**Table 2.** Freezing temperatures of binary sulphuric acid/water solution polluted with the particles graphite (gr), kaolin (ka), montmorillonite KSF (mKSF), montmorillonite K-10 (mK-10), respectively.

| $H_2SO_4$ [wt%] + (gr) | $T_{freeze}$ [°C] +/- 1°C | Volume [x $10^{-3}$ cm³] < +/- 5% |
|---|---|---|
| 5,6 ±0,2 | -12,6 | 3,0 |
| 5,7 ±0,2 | -21,6 | 5,0 |
| 5,8 ±0,2 | -18,3 | 4,1 |
| 5,8 ±0,2 | -22,2 | 3,8 |
| 5,9 ±0,3 | -22,6 | 4,6 |
| 6,1 ±0,2 | -27,7* | 4,3 |
| 6,2 ±0,2 | -11,5 | 4,1 |
| 6,3 ±0,2 | -21,1 | 2,2 |
| 6,4 ±0,2 | -20,2 | 3,6 |
| 6,4 ±0,3 | -16,7 | 2,4 |
| 6,4 ±0,3 | -22,4 | 3,9 |
| 6,6 ±0,2 | -23,5 | 4,0 |
| 6,8 ±0,3 | -31,4* | 3,0 |
| 11,8±0,5 | -26,1 | 4,1 |
| 11,8 ±0,5 | -28,1 | 3,9 |
| 11,9 ±0,5 | -27,5 | 3,6 |
| 12,0 ±0,4 | -25,1 | 4,3 |
| 12,1 ±0,4 | -25,4 | 2,8 |
| 12,4 ±0,5 | -29,5 | 3,4 |
| 12,6 ±0,5 | -30,7 | 3,4 |
| 12,9 ±0,5 | -27,8 | 3,6 |
| 13,4 ±0,5 | -31,4* | 4,1 |

| $H_2SO_4$ [wt%] + (mKSF) | $T_{freeze}$ [°C] +/- 1°C | Volume [x $10^{-3}$ cm³] < +/- 5% |
|---|---|---|
| 5,7±0,2 | -12,7 | 3,3 |
| 5,8 ±0,2 | -10,8 | 2,5 |
| 6,0 ±0,3 | -10,3 | 3,6 |
| 6,2 ±0,2 | -10,8 | 3,1 |
| 6,2 ±0,2 | -12,8 | 3,7 |
| 11,3 ±0,5 | -15,9 | 2,7 |
| 11,6 ±0,4 | -13,8 | 4,5 |
| 11,6 ±0,5 | -14,1 | 3,8 |
| 11,8 ±0,5 | -15,4 | 4,0 |
| 12,0 ±0,4 | -13,9 | 3,6 |
| 12,1 ±0,5 | -18,3 | 3,2 |
| 12,2 ±0,4 | -16,8 | 3,5 |
| 12,4 ±0,6 | -17,2 | 3,2 |
| 12,5 ±0,6 | -14,5 | 3,4 |
| 12,7 ±0,5 | -12,6 | 3,2 |



ACPD
4, 1887–1909, 2004

**Table 2.** Continued.

| $H_2SO_4$ [wt%] + (mK-10) | $T_{freeze}$ [°C] +/- 1°C | Volume [x $10^{-3}$ cm³] < +/- 5% |
|---|---|---|
| 5,7 ±0,3 | -22,1 | 2,2 |
| 6,0 ±0,3 | -23,3 | 2,8 |
| 6,1 ±0,2 | -13,6 | 5,8 |
| 6,1 ±0,2 | -28,8* | 2,7 |
| 6,1 ±0,2 | -27,9 | 4,1 |
| 6,4 ±0,2 | -25 | 3,0 |
| 6,5 ±0,3 | -24,2 | 3,7 |
| 11,3 ±0,5 | -10 | 3,9 |
| 11,6 ±0,4 | -15,3 | 4,0 |
| 11,7 ±0,5 | -24,1 | 5,6 |
| 11,9 ±0,5 | -26,2 | 3,1 |
| 12,2 ±0,5 | -31,1* | 3,6 |
| 12,2 ±0,5 | -26,4 | 4,2 |
| 12,7 ±0,5 | -19 | 4,3 |
| 13,1 ±0,5 | -33,1* | 3,5 |
| 13,6 ±0,5 | -24,1 | 3,1 |

| $H_2SO_4$ [wt%] + (ka) | $T_{freeze}$ [°C] +/- 1°C | Volume [x $10^{-3}$ cm³] < +/- 5% |
|---|---|---|
| 11,8 ±0,4 | -21,8 | 4,1 |
| 11,9 ±0,4 | -23,4 | 4,9 |
| 12,1 ±0,4 | -23,9 | 4,7 |
| 12,6 ±0,6 | -21,9 | 3,7 |
| 12,6 ±0,4 | -16,2 | 5,2 |
| 12,7 ±0,5 | -24,2 | 4,0 |
| 13,3 ±0,5 | -29,6* | 3,6 |
| 13,4 ±0,5 | -28,2* | 3,5 |
| 13,5 ±0,5 | -22 | 4,8 |
| 13,7 ±0,5 | -19,3 | 4,1 |
| 13,8 ±0,6 | -34,6* | 3,7 |

*These droplets contained only very few particles, so they could be frozen homogeneously an error in temperature of +/−1°C.



ACPD
4, 1887–1909, 2004

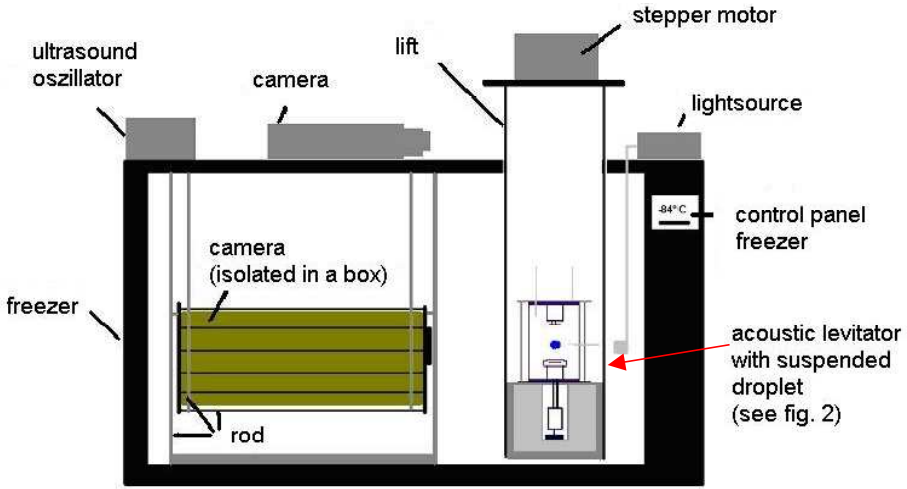


**Fig. 1.** Chest freezer with the movable acoustic levitator.



ACPD
4, 1887–1909, 2004

Heterogeneous freezing of single sulphuric acid solution droplets

M. Ettner et al.

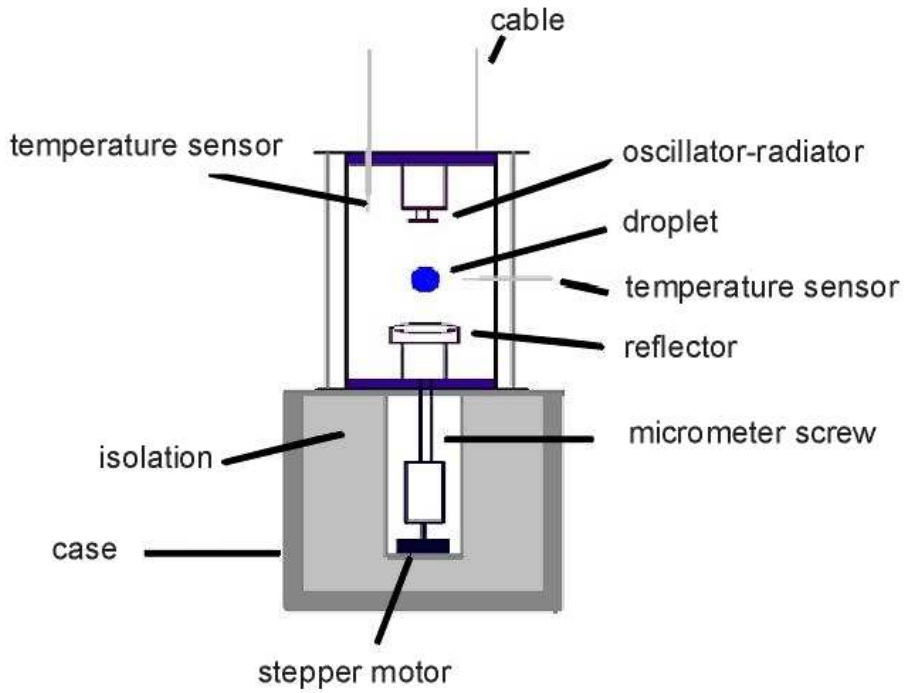


**Fig. 2.** Acoustic levitator with suspended droplet.



ACPD
4, 1887–1909, 2004

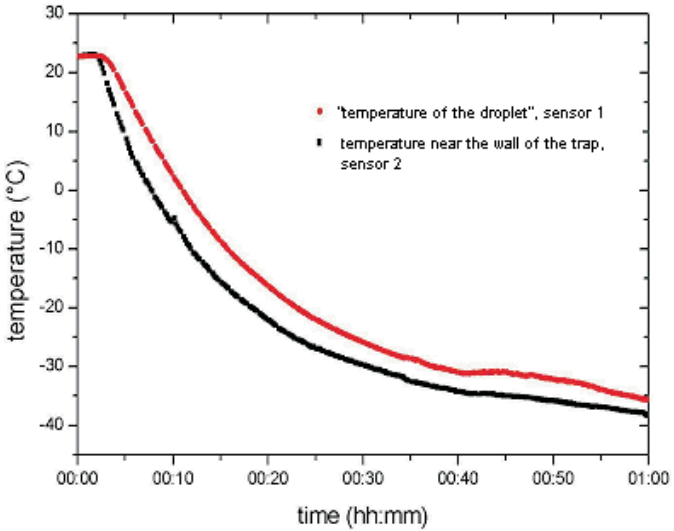


**Fig. 3.** Temperature decrease inside the plexiglass trap.



ACPD
4, 1887–1909, 2004

**Fig. 4.** Left: liquid droplet with a few graphite particles inside. Right: frozen droplet with graphite particles on the surface.



ACPD

4, 1887–1909, 2004

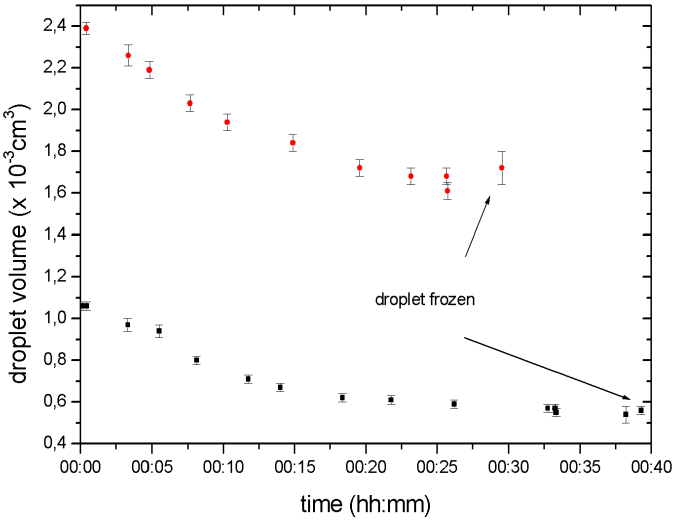


**Fig. 5. (a)** Volume decrease of two uncontaminated droplets with different initial size.



ACPD
4, 1887–1909, 2004

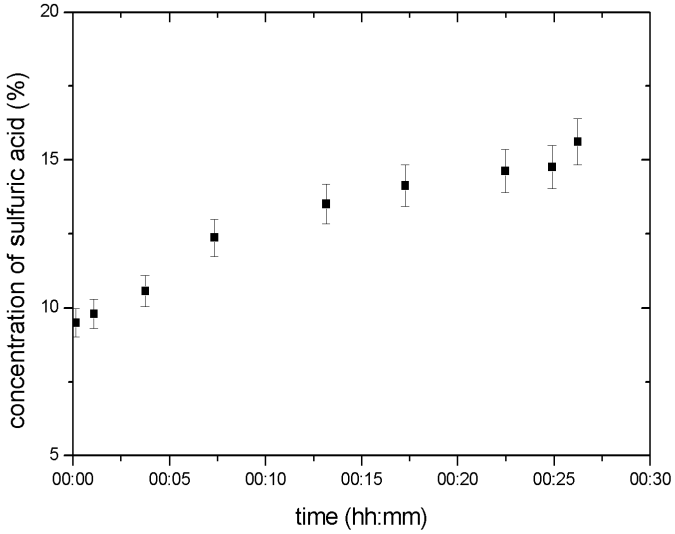


**Fig. 5. (b)** Increase of the sulphuric acid concentration.



ACPD
4, 1887–1909, 2004

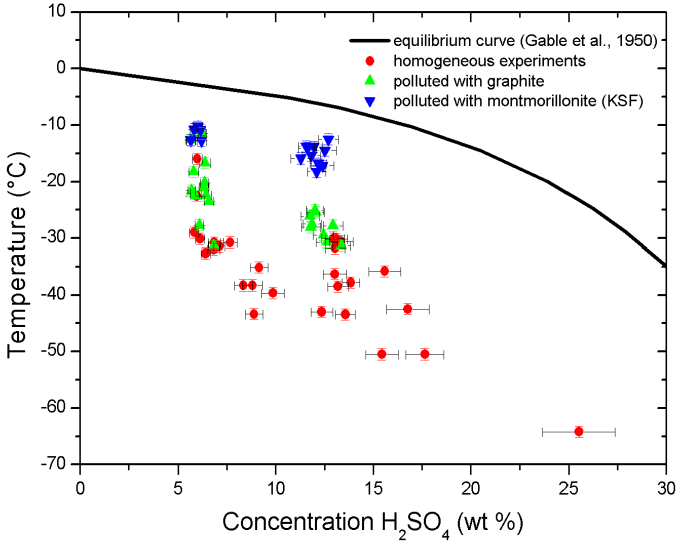


**Fig. 6.** Freezing temperatures of the sulphuric acid solution versus the concentration in wt %, droplets polluted with graphite and montmorillonite (KSF) compared to the pure solution together with the equilibrium ice melting curve (Gable et al., 1950).



ACPD
4, 1887–1909, 2004

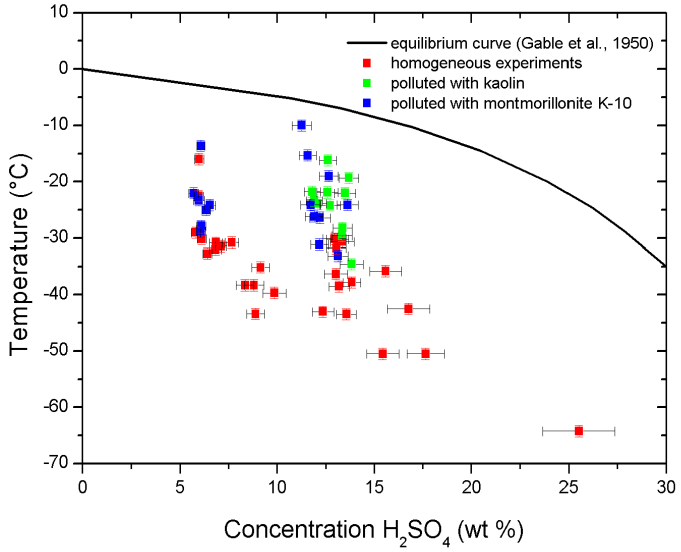


**Fig. 7.** Freezing temperatures of the sulphuric acid solution versus the concentration in wt %, droplets polluted with kaolin and montmorillonite (K-10) compared to the pure solution, together with the equilibrium ice melting curve (Gable et al., 1950).



ACPD
4, 1887–1909, 2004